X(5) Critical-Point Structure in a Finite System

A. Leviatan

Racah Institute of Physics, The Hebrew University, Jerusalem 91904, Israel

(Dated: February 9, 2008)

$X(5)$ is a paradigm for the structure at the critical point of a particular first-order phase transition for which the intrinsic energy surface has two degenerate minima separated by a low barrier. For a finite system, we show that the dynamics at such a critical point can be described by an effective deformation determined by minimizing the energy surface after projection onto angular momentum zero, and combined with two-level mixing. Wave functions of a particular analytic form are used to derive estimates for energies and quadrupole rates at the critical point.

PACS numbers: 21.60.Fw, 21.10.Re

Quantum phase transitions, occurring at zero temperature as a function of a coupling constant, have become a topic of great interest in different branches of physics [1, 2, 3]. Often this type of phase transition involves a structural change between different shapes or geometric configurations. Advanced experiments have identified such quantum shape-phase transitions in a variety of mesoscopic systems, with a finite number of constituents, *e.g.*, nuclei, molecules and atomic clusters. A key issue is to understand the modifications brought in by the finiteness of these systems near criticality. This question can be conveniently addressed in a class of quantum models in which the Hamiltonian is expanded in elements of a Lie algebra. Such models are widely used in the description of nuclei and molecules [4, 5]. In the present work we study this question in connection with nuclei, exemplifying a finite system undergoing a first-order shape-phase transition. The tools developed are applicable to other mesoscopic systems described by similar models albeit with different spectrum generating algebras.

Recently, it has been recognized that quantum shape-phase transitions are amenable to analytic descriptions at the critical points [1, 2]. The importance of these analytic benchmarks of criticality lies in the fact that they provide a classification of states and analytic expressions for observables in regions where the structure changes most rapidly. For nuclei these benchmarks were obtained in the geometric framework of a Bohr Hamiltonian for macroscopic quadrupole shapes. In particular, the E(5) [1] (X(5) [2]) benchmark is applicable to a second- (first-) order phase transition between spherical and deformed γ-unstable (axially-symmetric) nuclei. In the present work we focus on the X(5) benchmark for which an empirical example has been found in ^{152}Sm, ^{150}Nd, ^{156}Dy and ^{154}Gd [6, 7, 8, 9]. The role of a finite number of nucleons can be addressed in the algebraic framework of the interacting boson model (IBM) [4] which describes low-lying quadrupole collective states in nuclei in terms of a system of N monopole (s) and quadrupole (d) bosons representing va-

lence nucleon pairs. The model has U(6) as a spectrum generating algebra and its three dynamical symmetry limits: U(5), SU(3), and O(6), describe the dynamics of stable nuclear shapes: spherical, axially-deformed, and γ-unstable deformed. Phase transitions for finite N are studied by an IBM Hamiltonian involving terms from different dynamical symmetry chains [10]. An important conclusion from many such studies [11, 12, 13, 14, 15, 16, 17] is that although in finite systems the discontinuities at the critical point are smoothed out, features of the phase transition persist even at moderate values of N ($N = 10$ for ^{152}Sm).

The original formulation of the E(5) and X(5) models [1, 2] employed an infinite square-well potential in the β variable of the Bohr Hamiltonian. This is an adequate approximation for an E(5)-like second-order phase transition, where the relevant potential is γ-indpendent and flat-bottomed. This behaviour persists in the finite-N energy surface, obtained by the method of coherent states [10, 18]. In this case, the large fluctuations in β can be taken into account by means of an effective β-deformation determined by minimizing the energy surface after projection onto the appropriate $[O(5)]$ symmetry [14]. The structure of X(5)-like first-order phase transition is more complex. The geometric $X(5)$ solution [2] assumes the decoupling of the β and γ degrees of freedom. The corresponding finite-N energy surface displays two degenerate minima separated by a low barrier. Analysis of the IBM wave functions near the critical-point show clear evidence for phase coexistence and level crossing [11, 13, 15]. This indicates that although the barrier between the two minima is small, its effect cannot be completely ignored. In the present work we examine the conditions for and properties of $X(5)$ critical-point structure in a finite system.

Focusing on the dynamics of the β degree of freedom, in the geometric approach, the X(5) eigenfunctions [2] are proportional to Bessel functions, and the spectrum consists of families of states, L^+_ξ, labeled by $\xi = 1, 2, \ldots$, with angular momentum $L = 0, 2, 4, \ldots$ and projection $K = 0$ along the symmetry-axis. The X(5) benchmark leads to analytic parameter-free

predictions for energy ratios and $B(E2)$ ratios which, as seen in Table I, are in-between the values expected of a spherical vibrator [$U(5)$] and an axially-deformed rotor [$SU(3)$].

In the algebraic approach, the $U(5)$-$SU(3)$ transition is modeled by the Hamiltonian

$$H \;=\; \epsilon\,\hat{n}_d - \kappa\,Q\cdot Q\;. \tag{1}$$

Here $\hat{n}_d$ is the d-boson number operator, Q is the quadrupole generator of $SU(3)$ and the dot implies a scalar product. In the $U(5)$ limit ($\kappa = 0$), the spectrum of H is harmonic, and the eigenstates are classified according to the chain $U(6) \supset U(5) \supset O(5) \supset O(3)$ with quantum numbers $|\,N, n_d, \tau, L\rangle$ (for $\tau \geq 6$ an additional multiplicity index may be required for complete classification). In the $SU(3)$ limit ($\epsilon = 0$), the Hamiltonian is related to the Casimir operator of $SU(3)$ and the spectrum is indicated in the caption of Table I. The eigenstates are classified according to the chain $U(6) \supset SU(3) \supset O(3)$ with quantum numbers $|\,N, (\lambda,\mu), K, L\rangle$. A geometric visualization is obtained by an intrinsic energy surface defined by the expectation value of the Hamiltonian in the coherent state [10, 18]

$$|\,\beta,\gamma; N\rangle \;=\; (N!)^{-1/2}(b_c^\dagger)^N\,|0\,\rangle\;, \tag{2}$$

where $b_c^\dagger = (1+\beta^2)^{-1/2}[\beta\cos\gamma\, d_0^\dagger + \beta\sin\gamma\,(d_2^\dagger + d_{-2}^\dagger)/\sqrt{2} + s^\dagger]$ with $\beta \geq 0$ and $0 \leq \gamma \leq \pi/3$.

The IBM Hamiltonian at the critical point of the $U(5)$-$SU(3)$ phase transition corresponds to the following choice of parameters [10] in the Hamiltonian of Eq. (1)

$$\epsilon \;=\; \frac{9}{4}\kappa(2N-3)\;. \tag{3}$$

Its intrinsic energy surface given by

$$E(\beta,\gamma) \;=\; -5\kappa N + \frac{\kappa\,N(N-1)\,\beta^2}{2(1+\beta^2)^2}\left(1 - 4\sqrt{2}\beta\cos 3\gamma + 8\beta^2\right), \tag{4}$$

has the typical form of a Landau potential for a first-order phase transition, with two degenerate minima, at $\beta = 0$ and at ($\beta = \frac{1}{2\sqrt{2}}, \gamma = 0$). As shown in Fig. (1), the barrier

separating the spherical and prolate-deformed minima is extremely small and the resulting surface, $E(\beta) \equiv E(\beta, \gamma = 0)$, is rather flat. This behaviour motivated the use of a square-well potential in the X(5) model [2]. Guided by the experience gained with finite-N flat-bottomed potentials in second-order phase transitions [14], we are led to consider states, $|\,\beta; N, L\rangle$, of good $O(3)$ symmetry L projected from the intrinsic state $|\beta, \gamma = 0; N\rangle$ of Eq. (2), with an effective β-deformation yet to be determined. In the $U(5)$ basis these L-projected states are

$$|\,\beta; N, L\rangle \;=\; \sum_{n_d,\tau} \frac{1}{2}\left[1 + (-1)^{n_d-\tau}\right]\, \xi^{(N,L)}_{n_d,\tau} |\, N, n_d, \tau, L\rangle \;, \tag{5}$$

where L is even, τ takes the values compatible with the $O(5) \supset O(3)$ reduction and the n_d summation covers the range $\tau \leq n_d \leq N$. The coefficients $\xi^{(N,L)}_{n_d,\tau}$ are of the form

$$\xi^{(N,L)}_{n_d,\tau} \;=\; \left[\Gamma^{(L)}_N(\beta)\right]^{-1/2} f^{(L)}_\tau \frac{\beta^{n_d}}{\left[(N-n_d)!(n_d-\tau)!!(n_d+\tau+3)!!\right]^{1/2}} \tag{6}$$

where $\Gamma^{(L)}_N(\beta)$ is a normalization factor. In some cases analytic expressions of these coefficients can be derived. Specifically, for $L = 0$: $f^{(0)}_\tau = (-1)^\tau\sqrt{2\tau+3}$ with $\tau = 0, 3, 6, \ldots$ and for $L = 2$: $f^{(2)}_\tau = (-1)^{\tau+1}\sqrt{\tau+2}$ $(= (-1)^{\tau+1}\sqrt{\tau+1}\,)$ with $\tau = 1, 4, 7, \ldots$ (with $\tau = 2, 5, 8, \ldots$). In general, $\xi^{(N,L)}_{n_d,\tau}$ can be obtained by numerical diagonalization of Hamiltonians which have the condensate (2) as an exact eigenstate [19]. The states $|\,\beta; N, L\rangle$ interpolate between the $U(5)$ spherical ground state, $|s^N\rangle$, with $n_d = \tau = L = 0$, at $\beta = 0$, and the $SU(3)$ deformed ground band with $(\lambda, \mu) = (2N, 0)$, at $\beta = \sqrt{2}$. For arbitrary β the matrix elements of the Hamiltonian in these states define an L-projected energy surface [20], $E^{(N)}_L(\beta) = \langle\beta; N, L|H|\beta; N, L\rangle$, which can be evaluated in closed form

$$\begin{aligned} E^{(N)}_L(\beta) \;=\; & \epsilon\left[\, N - S^{(N)}_{1,L}\,\right] \\ & + \frac{1}{2}\kappa\left[\,(\beta^2-2)^2\, S^{(N)}_{2,L} + 2(\beta-\sqrt{2})^2\,\Sigma^{(N)}_{2,L} + \frac{3}{4}L(L+1) - 2N(2N+3)\,\right] . \end{aligned} \tag{7}$$

The quantities $S^{(N)}_{1,L}$, $S^{(N)}_{2,L}$ and $\Sigma^{(N)}_{2,L}$ are, respectively, the expectation values of $\hat{n}_s = s^\dagger s$, $(s^\dagger)^2 s^2$ and $\hat{n}_s\,\hat{n}_d$ in the states $|\beta; N, L\rangle$. They are determined by the normalization factor

$\Gamma_N^{(L)}(\beta)$ of Eq. (6)

$$S_{1,L}^{(N)} \;=\; \frac{\Gamma_{N-1}^{(L)}(\beta)}{\Gamma_N^{(L)}(\beta)} \;, \tag{8}$$

with $S_{2,L}^{(N)} = S_{1,L}^{(N)} S_{1,L}^{(N-1)}$ and $\Sigma_{2,L}^{(N)} = (N-1)S_{1,L}^{(N)} - S_{2,L}^{(N)}$.

As noted in [21] and shown in Fig. (1b), the $L = 0$ projected energy surface, $E_{L=0}^{(N)}(\beta)$, no-longer exhibits the double minima structure observed in the (unprojected) intrinsic energy surface. Instead, there is a minimum at $\beta > 0$, a maximum at $\beta = 0$, and a saddle point in the γ direction at $\beta < 0$. $E_{L=2}^{(N)}(\beta)$ resembles the potential used in the geometric collective model calculation of ^{152}Sm [22] with a minimum at a larger value of $\beta > 0$, and a flat shoulder near $\beta = 0$. The different behaviour of $E_{L=2}^{(N)}(\beta)$ and $E_{L=0}^{(N)}(\beta)$ can be attributed to the fact that, as shown in Fig. (1a), the $L = 2$ state is well above the barrier and hence experiences essentially a flat-bottomed potential. In contrast, the two minima in the intrinsic energy surface support two coexisting $L = 0$ states which, in view of the low barrier, are subject to considerable mixing. The mixing between the spherical and deformed $L = 0$ states

$$\begin{aligned} |\phi_1\rangle \;&\equiv\; |s^N\rangle \;, \\ |\phi_2\rangle \;&\equiv\; |\beta; N, L=0\rangle \;, \end{aligned} \tag{9}$$

can be studied by means of a 2×2 potential energy matrix, $m_{ij} = \langle\phi_i|H|\phi_j\rangle$, given by

$$\begin{aligned} m_{11} \;&=\; -5\kappa\, N \;\;,\;\; m_{12} = -\kappa N \left[\beta^2(N-1) + 5\right] r_{12} \;, \\ m_{22} \;&=\; E_{L=0}^{(N)}(\beta) \;\;,\;\; r_{12} = \left[N!\,\Gamma_N^{(L=0)}(\beta)\right]^{-1/2} \;, \end{aligned} \tag{10}$$

where $r_{12} = \langle\phi_1|\phi_2\rangle$ is the overlap. The eigenpotentials are obtained by diagonalization and the equilibrium β-deformation is determined from the minimum of the lowest eigenpotential. This procedure is in the spirit of the matrix coherent-state approach proposed in [23] to describe the geometry of configuration mixing in nuclei. An important difference being that instead of using coherent states with different values of N, in the present study we consider

states with good angular momentum, $L = 0$, and fixed N. A slight complication arises from the fact the two states $|\phi_1\rangle$ and $|\phi_2\rangle$ are not orthogonal. This can be taken into account by transforming into an orthonormal basis of $L = 0$ states

$$\begin{aligned} |\Psi_1\rangle &= |\phi_1\rangle \ , \\ |\Psi_2\rangle &= (1 - r_{12}^2)^{-1/2} \ (\, |\phi_2\rangle - r_{12} \, |\phi_1\rangle \,) \ . \end{aligned} \tag{11}$$

The matrix elements $K_{ij} = \langle \Psi_i | H | \Psi_j \rangle$ are then given by

$$\begin{aligned} K_{11} &= m_{11} \ , \ K_{12} = (1 - r_{12}^2)^{-1/2} \, (\, m_{12} - r_{12} \, m_{11} \,) \\ K_{22} &= (1 - r_{12}^2)^{-1} \left(m_{22} - 2 r_{12} \, m_{12} + r_{12}^2 \, m_{11} \right) \ . \end{aligned} \tag{12}$$

The eigenvalues define the eigenpotentials

$$\begin{aligned} E_{L=0}^{(\pm)}(\beta) &= \left(K_{11} + K_{22} \pm \Delta \right) / 2 \ , \\ \Delta &= \sqrt{(K_{22} - K_{11})^2 + 4 K_{12}^2} \ , \end{aligned} \tag{13}$$

and the corresponding eigenvectors are given by

$$\begin{aligned} |\Phi_{L=0}^{(-)}\rangle &= \sin\theta \, |\Psi_1\rangle + \cos\theta \, |\Psi_2\rangle \ , \\ |\Phi_{L=0}^{(+)}\rangle &= \cos\theta \, |\Psi_1\rangle - \sin\theta \, |\Psi_2\rangle \ , \\ \tan\theta &= \frac{2 K_{12}}{K_{22} - K_{11} - \Delta} \ . \end{aligned} \tag{14}$$

The lowest eigenpotential, $E_{L=0}^{(-)}(\beta)$, is shown in Fig. (1b) for $N = 10$. It has a minimum at a value of $\beta = 0.591$, larger than the minimum ($\beta = 0.528$) of the (unmixed) $L = 0$ projected energy surface and in close proximity to the minimum ($\beta = 0.619$) of the $L = 2$ projected energy surface. We now identify the members of the ground band ($\xi = 1$) as $|0_1^+\rangle = |\Phi_{L=0}^{(-)}\rangle$, Eq. (14), with energy $E_{L=0}^{(-)}(\beta)$, Eq. (13), and for $L > 0$ even, $|L_1^+\rangle = |\beta; N, L\rangle$, Eq. (5), with energy $E_L^{(N)}(\beta)$, Eq. (7). The bandhead of the first excited band ($\xi = 2$) corresponds to

$|0_2^+\rangle = |\Phi^{(+)}_{L=0}\rangle$, Eq. (14), with energy $E^{(+)}_{L=0}(\beta)$, Eq. (13). The value of β used in the indicated wave functions and energies is chosen at the global minimum of $E^{(-)}_{L=0}(\beta)$.

Having at hand explicit expressions for the wave functions, we can evaluate $E2$ matrix elements. To conform with the geometric $X(5)$ model [2], we employ an IBM quadrupole operator, $T(E2) = d^\dagger s + s^\dagger \tilde{d}$, linear in the deformation. For transitions involving the $L = 0_1^+$, 2_1^+ and 0_2^+ states, analytic expressions can be derived for $B(E2)$ values by means of the matrix elements $T_1 \equiv \langle \beta; N, L' = 2 || \, T(E2) \, || \beta; N, L = 0 \rangle$ and $T_2 \equiv \langle \beta; N, L' = 2 || \, T(E2) \, || s^N \rangle$,

$$
\begin{aligned}
T_1 &= \frac{\beta \left[\Gamma^{(2)}_{N-1}(\beta) + \Gamma^{(0)}_{N-1}(\beta) \right]}{\left[\Gamma^{(2)}_{N}(\beta) \, \Gamma^{(0)}_{N}(\beta) \right]^{1/2}} \, , \\
T_2 &= \frac{\beta N}{\left[N! \, \Gamma^{(2)}_{N}(\beta) \, \right]^{1/2}} \, .
\end{aligned}
\tag{15}
$$

To test the suggested procedure we compare in Table II the $U(5)$ decomposition of exact eigenstates obtained from numerical diagonalization of the critical Hamiltonian, Eq. (3), for $N = 10$, with that calculated using the L-projected states with $\beta = 0.591$ [the global minimum of $E^{(-)}_{L=0}(\beta)$]. As can be seen, the latter provide an accurate approximation to the exact eigenstates for yrast states (the overlaps between calculated and exact states are 99.6, 99.1, 98.0, 97.0, 96.6, 96.65 % for $L = 0_1^+$, 2_1^+, 4_1^+, 8_1^+, 10_1^+, respectively). This agreement in the structure of wave functions is translated also into an agreement in energies and B(E2) values as shown in Table I. For the $L = 0_2^+$ state, the agreement is fair but less precise, in view of the smaller overlap (81.9%). It appears that this non-yrast state is affected by additional states beyond the two-state mixing considered here. The results of Table I and II clearly demonstrate the ability of the suggested procedure to provide faithful estimates to the exact finite-N calculations of the critical IBM Hamiltonian, which in-turn capture the essential features of the $X(5)$ critical-point structure relevant to ^{152}Sm (which is slightly past the phase transition towards $SU(3)$ [6]).

To summarize, we have examined the structure at the $X(5)$ critical-point of a first-

order shape-phase transition in a finite system, by means of an effective β-deformation, determined by variation after L-projection and two-level mixing. The same procedure can be used throughout the coexistence region, where the two minima in the potential coexist but are not necessarily degenerate. In this case, the control parameter κ/ϵ in Eq. (1) spans the range between the spinodal point (where the second minimum shows up) and the antispinodal point (where the first minimum disappears), which embrace the critical point. Although we have treated explicitly the case of atomic nuclei described by the IBM, the same approach is applicable to first-order phase transitions in other mesoscopic systems, such as polyatomic molecules described by the algebraic vibron model [5]. This work was supported by the Israel Science Foundation.

[1] F. Iachello, Phys. Rev. Lett. **85**, 3580 (2000).

[2] F. Iachello, Phys. Rev. Lett. **87**, 052502 (2001).

[3] M. Vojta, Rep. Prog. Phys. **66**, 2069 (2003).

[4] F. Iachello and A. Arima, *The Interacting Boson Model* (Cambridge Univ. Press, 1987).

[5] F. Iachello and R.D. Levine, *Algebraic Theory of Molecules* (Oxford Univ. Press, 1994).

[6] R.F. Casten and N.V. Zamfir, Phys. Rev. Lett. **87**, 052503 (2001).

[7] R. Krücken *et al.*, Phys. Rev. Lett. **88**, 232501 (2002).

[8] M.A. Caprio, *et al.*, Phys. Rev. C **66**, 054310 (2002).

[9] D. Tonev *et al.*, Phys. Rev. C **69**, 034334 (2004).

[10] A.E.L. Dieperink, O. Scholten and F. Iachello, Phys. Rev. Lett. **44**, 1747 (1980).

[11] F. Iachello, N.V. Zamfir and R.F. Casten, Phys. Rev. Lett. **81**, 1191 (1998).

[12] R.F. Casten, D. Kusnezov and N.V. Zamfir, Phys. Rev. Lett. **82**, 5000 (1999).

[13] N.V. Zamfir, P. von Brentano, R.F. Casten and J. Jolie, Phys. Rev. C **66**, 021304(R) (2002).

[14] A. Leviatan and J.N. Ginocchio, Phys. Rev. Lett. **90**, 212501 (2003).

[15] J.M. Arias, J. Dukelsky and J.E. García-Ramos, Phys. Rev. Lett. **91**, 162502 (2003).

[16] F. Iachello and N.V. Zamfir, Phys. Rev. Lett. **92**, 212501 (2004).

[17] D.J. Rowe, P.S. Turner and G. Rosensteel, Phys. Rev. Lett. **93**, 232502 (2004).

[18] J.N. Ginocchio and M.W. Kirson, Phys. Rev. Lett. **44**, 1744 (1980).

[19] M.W. Kirson and A. Leviatan, Phys. Rev. Lett. **55**, 2846 (1985).

[20] K. Hagino, G.F. Bertsch and P.-G. Reinhard, Phys. Rev. C **68**, 024306 (2003).

[21] J. Jolie, P. Cejnar and J. Dobeš, Phys. Rev. C **60**, 061303(R) (1999).

[22] Jing-ye Zhang, M.A. Caprio, N.V. Zamfir and R.F. Casten, Phys. Rev. C **60**, 061304(R) (1999).

[23] A. Frank, P. Van Isacker and C.E. Vargas, Phys. Rev. C **69**, 034323 (2004).

TABLE I: Excitation energies (in units of $E(2_1^+) = 1$) and B(E2) values (in units of $B(E2; 2_1^+ \rightarrow 0_1^+) = 1$) for the X(5) critical-point benchmark [2], for several N=10 calculations, and for the experimental data of ^{152}Sm [6]. The finite-N calculations involve the exact diagonalization of the critical IBM Hamiltonian [Eq. (3)], L-projected states [Eqs. (7), (13) and (15) with $\beta = 0.591$], the $U(5)$ limit $[\epsilon\, n_d]$ and the $SU(3)$ limit $(\kappa/2)[-\lambda^2 - \mu^2 - \lambda\mu - 3\lambda - 3\mu + 3L(L+1)/4]$.

	X(5)	exact N=10	L-projection N=10	$U(5)$ N=10	$SU(3)$ N=10	^{152}Sm exp
$E(4_1^+)$	2.91	2.43	2.46	2	3.33	3.01
$E(6_1^+)$	5.45	4.29	4.33	3	7.00	5.80
$E(8_1^+)$	8.51	6.53	6.56	4	12.00	9.24
$E(10_1^+)$	12.07	9.12	9.13	5	18.33	13.21
$E(0_2^+)$	5.67	2.64	3.30	2	25.33	5.62
$4_1^+ \rightarrow 2_1^+$	1.58	1.61	1.60	1.8	1.40	1.45
$6_1^+ \rightarrow 4_1^+$	1.98	1.85	1.80	2.4	1.48	1.70
$8_1^+ \rightarrow 6_1^+$	2.27	1.92	1.87	2.8	1.45	1.98
$10_1^+ \rightarrow 8_1^+$	2.61	1.87	1.86	3.0	1.37	2.22
$0_2^+ \rightarrow 2_1^+$	0.63	0.78	0.61	1.8	0.07	0.23

TABLE II: $U(5)$ decomposition (in %) of yrast L_1^+ states for $N = 10$. The exact values are obtained from numerical diagonalization of the critical IBM Hamiltonian, Eq. (3). The calculated values are obtained from the L-projected states, Eqs. (6) and (14) with $\beta = 0.591$.

	0_1^+		2_1^+		4_1^+			6_1^+		8_1^+		10_1^+	
(n_d,τ)	exact	calc	exact	calc	exact	calc	(n_d,τ)	exact	calc	exact	calc	exact	calc
(0,0)	52.3	52.0					(3,3)	43.0	54.1				
(1,1)			41.8	41.1			(4,4)	23.9	26.4	46.9	60.1		
(2,0)	31.65	30.15					(5,3)	19.25	12.6				
(2,2)			13.5	18.4	40.8	47.8	(5,5)	2.3	2.1	26.7	26.5	52.2	66.2
(3,1)			26.5	25.7			(6,4)	7.7	3.7	15.5	8.45		
(3,3)	5.2	8.0			19.8	24.25	(6,6)	0.4	0.2	3.1	2.3	28.1	25.1
(4,0)	7.9	7.35					(7,3)	2.2	0.6				
(4,2)			7.3	7.0	22.9	18.1	(7,5)	0.5	0.2	5.8	2.15	11.7	5.4
(4,4)			2.3	2.5	1.1	1.3	(7,7)	0.2	0.1	0.2	0.1	3.4	2.05
(5,1)			5.75	3.7			(8,4)	0.5	0.1	1.1	0.2		
(5,3)	1.8	1.9			8.6	5.6	(8,6)	0.05	0.0	0.4	0.1	3.7	1.1
(5,5)			0.4	0.4	1.0	0.7	(8,8)	0.0	0.0	0.1	0.0	0.1	0.0
(6,0)	0.8	0.5					(9,3)	0.05	0.0				
(6,2)			1.1	0.6	3.8	1.5	(9,5)	0.0	0.0	0.2	0.0	0.4	0.05
(6,4)			0.6	0.35	0.3	0.2	(9,7)	0.0	0.0	0.0	0.0	0.2	0.0
(6,6)	0.05	0.05			0.3	0.2							
(7,1)			0.4	0.1									
(7,3)	0.2	0.1			0.9	0.3							
(7,5)			0.1	0.0	0.2	0.05							
(8,2)			0.05	0.0	0.2	0.0							

FIG. 1: Energy surfaces of the critical IBM Hamiltonian, Eq. (3), with $\kappa = 0.2$ and $N = 10$. (a) Intrinsic energy surface $E(\beta) \equiv E(\beta, \gamma = 0)$, Eq. (4), [solid line]. The unmixed $L = 0$ and $L = 2$ levels are shown for illustration. (b) $E(\beta)$ [solid line] as in (a), unmixed $L = 0$ [dashed line] and $L = 2$ [long dashed line] projected energy surfaces, $E_L(\beta) \equiv E_L^{(N)}(\beta)$, Eq. (7), and the lowest $L = 0$ eigenpotential [dot-dashed line], $E_{L=0}^{(-)}(\beta)$, Eq. (13), whose global minimum is at $\beta = 0.591$.

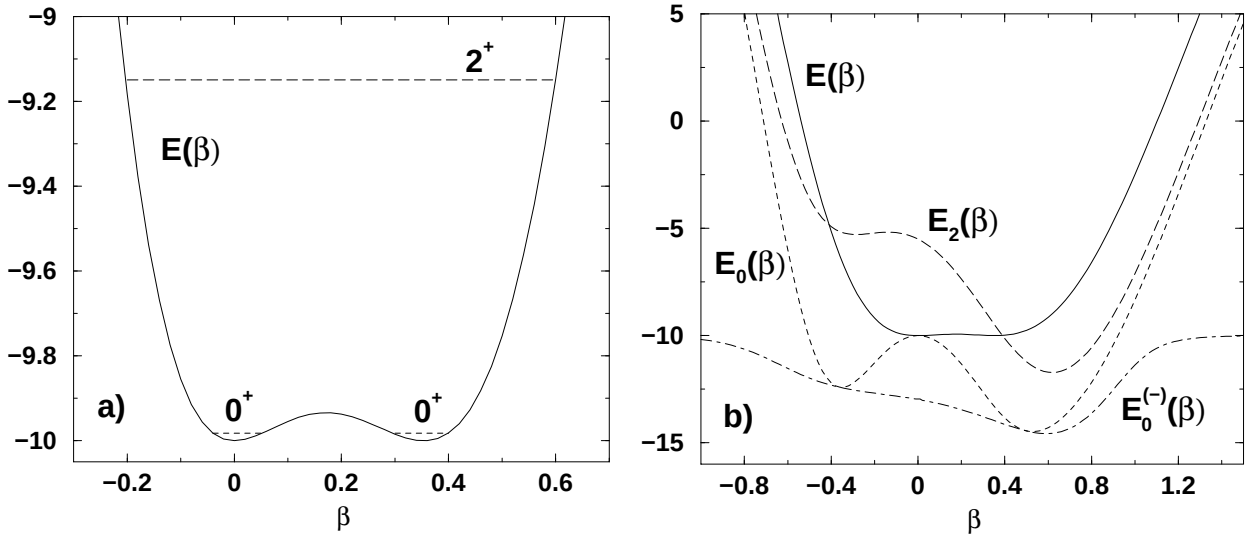
−9
−9.2
−9.4
−9.6
−9.8
−10
2+
E(β)
a)
0+
0+
−0.2
0
0.2
0.4
0.6
β
5
0
−5
−10
−15
E(β)
E2(β)
E0(β)
b)
E0(−)(β)
−0.8
−0.4
0
0.4
0.8
1.2
β

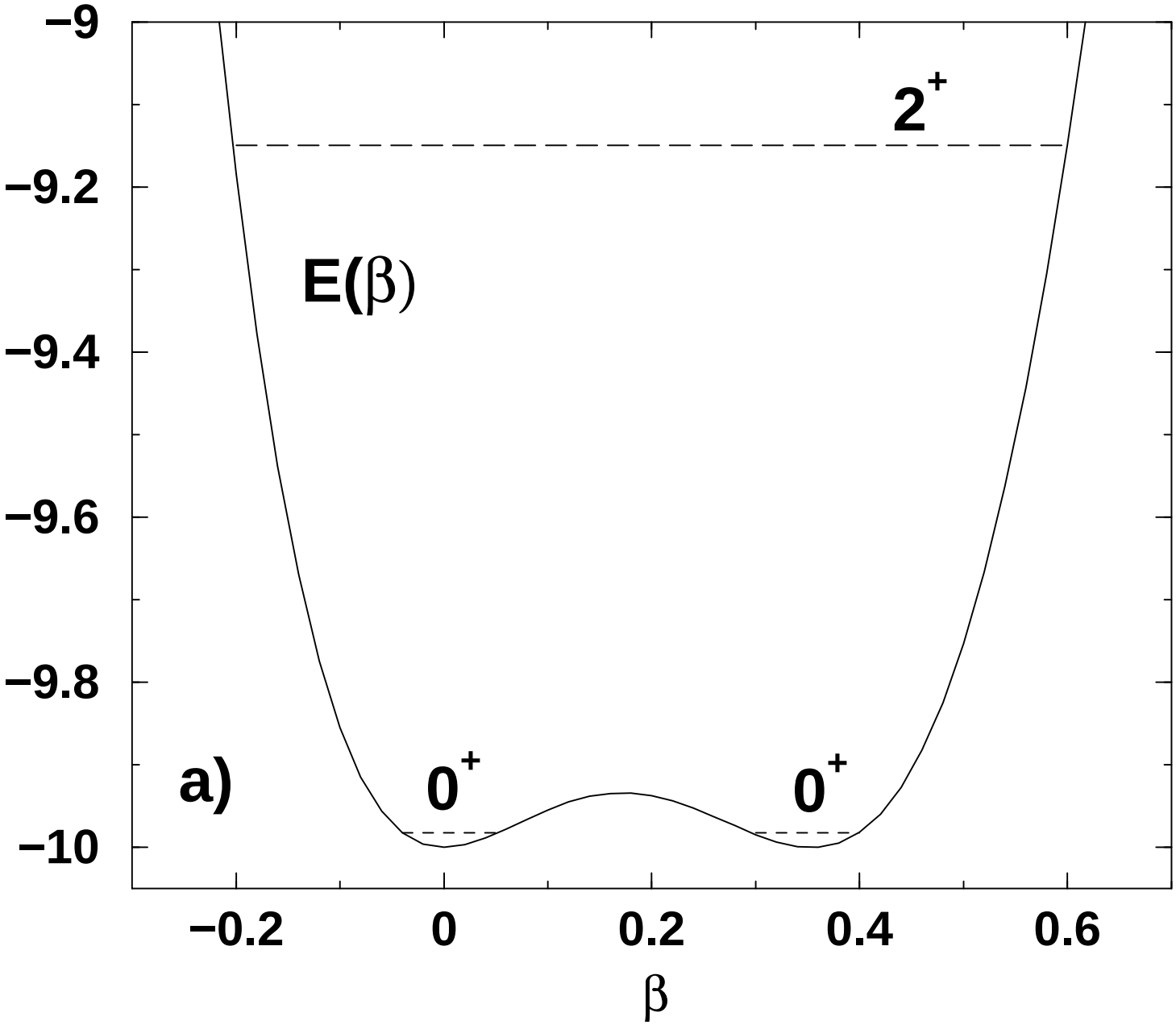
−9
−9.2
−9.4
−9.6
−9.8
−10
2+
E(β)
a)
0+
0+
−0.2
0
0.2
0.4
0.6
β

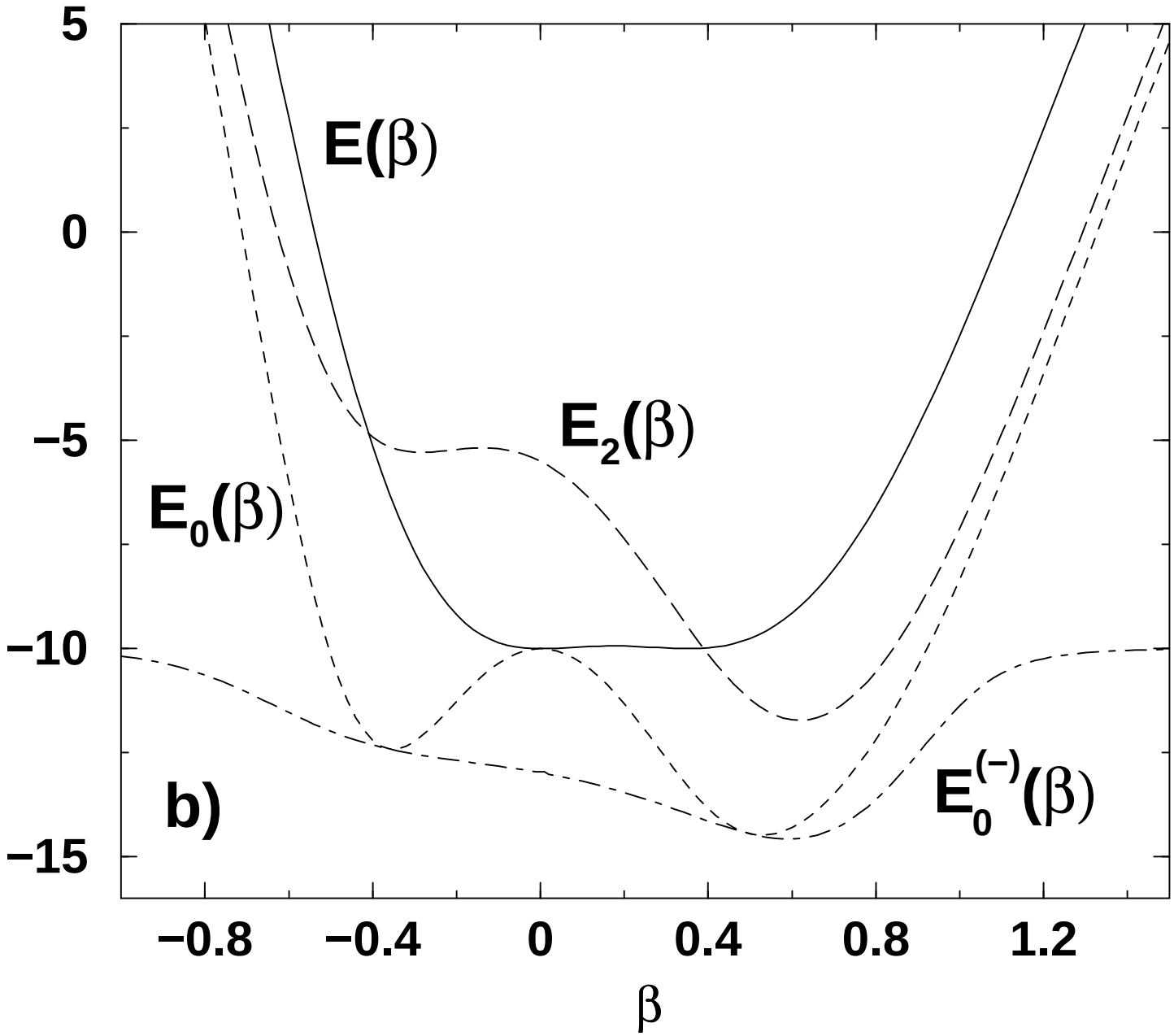
5
0
−5
−10
−15
−0.8
−0.4
0
0.4
0.8
1.2
β
E(β)
E2(β)
E0(β)
E0(−)(β)
b)